Conformational Behavior of *Escherichia coli* OmpA Signal Peptides in Membrane Mimetic Environments†

Josep Rizo,‡ Francisco J. Blanco,‡,§ Bostjan Kobe,‖ Martha D. Bruch,‡,⊥ and Lila M. Gierasch*,‡,‖

Departments of Pharmacology and Biochemistry, University of Texas Southwestern Medical Center, 5323 Harry Hines Boulevard, Dallas, Texas 75235-9041

Received October 21, 1992; Revised Manuscript Received February 26, 1993

ABSTRACT: Nuclear magnetic resonance and circular dichroism (CD) studies of isolated peptides corresponding to WT and mutant OmpA signal sequences are reported; all of the peptides adopt substantial amounts of α-helical structure both in 1:1 (v/v) trifluoroethanol (TFE)/water and in sodium dodecyl sulfate (SDS) micelles. In TFE/water, the helix begins after the positively charged N-terminal residues and is most stable in the hydrophobic core, which correlates with results obtained previously for other signal sequences. The helix is weaker between the hydrophobic core and the C-terminus; such a break in the helix appears to be common to other signal peptides studied previously and could be of functional importance. No clear correlation could be established between the helicity of the peptides in TFE/water and their in vivo activities. All the peptides have a higher α-helix content in SDS than in TFE/water, and there is a good correlation between helix content in SDS and in vivo activity. Helicity in SDS for the functional peptides increases both at the N-terminus and in the hydrophobic core, and is driven by a strong association of the core with the hydrophobic chains of the detergent. The extension of the helix toward the N-terminus may be a result of neutralization of the N-terminal positive charges by the headgroups of the micelles, which removes unfavorable electrostatic interactions with the helix dipole. All these comparisons were facilitated by the use of upfield shifts of Hα protons in helical regions relative to random coil chemical shifts, which also yielded estimates of helical content that correlated well with the CD results.

Most secreted proteins are synthesized with an N-terminal extension that signals their extracellular destination. These extensions, termed signal or leader sequences, are 15–30 residues long and in most cases are cleaved from the mature part of the protein after translocation [for recent reviews, see Briggs and Gierasch (1986), Verner and Schatz (1988), Gierasch (1989), Randall and Hardy (1989), Gennity et al. (1990), and Schatz and Beckwith (1990)]. Genetic, biochemical, and biophysical studies have afforded a wealth of information on the properties of signal sequences and their possible involvement in different steps of the export process. Signal sequences appear to interact with several proteins of the export apparatus, such as SecA, SecE, and SecY in prokaryotes (Bieker et al. 1990; Hartl et al., 1990), or the signal recognition particle in eukaryotes (Siegel & Walter, 1988; Rapoport, 1990). Several lines of evidence also point to a direct interaction between signal sequences and membrane lipids (Geller & Wickner, 1985; Briggs et al., 1985, 1986; de Vrije et al., 1988; Jones et al., 1990; Killian et al., 1990a). However, the roles of signal sequences in the export mechanism(s) are still far from being well understood. In particular, little is known about the involvement of signal sequences in the actual translocation step, and it has been difficult to obtain experimental evidence to test hypotheses based on proteinaceous membrane pores (Blobel & Doberstein, 1975; Blobel, 1980; Rapoport, 1986; Simon & Blobel, 1992), or on direct passage through the membrane lipids (von Heijne & Blomberg, 1979; Wickner, 1980; Inouye & Halegoua, 1980; Engelman & Steitz, 1981).

Signal sequences are characterized by a polar, positively charged N-terminus, followed by a 7–13-residue-long hydrophobic core, and a less apolar C-terminus that contains the cleavage site (von Heijne, 1985). The importance of these general characteristics for function has been stressed by the successful design of idealized signal sequences with hydrophobic cores containing only Leu or Ile residues (Kendall et al., 1986; Kendall & Kaiser, 1988; Yamamoto et al., 1987). The fact that signal peptide function is governed by a charge/hydrophobicity pattern rather than by a specific residue sequence makes signal sequences ideal targets for biophysical characterization, and studies of isolated signal peptides have revealed well-defined correlations between their biophysical properties and their ability to function in vivo (Jones et al., 1990). Several studies with isolated signal peptides have shown that they have high affinity for model lipid membranes and can penetrate into their acyl chain region (Briggs et al., 1985; Batenburg et al., 1988a; McKnight et al., 1991). This affinity decreases in functionally defective mutants with lower hydrophobicity in the hydrophobic core (McKnight et al., 1989), and also depends on the lipid composition (Killian et al., 1990b). The interaction of signal peptides with model membranes appears to affect the organization of the lipid assembly, and such perturbation could be critical for protein translocation (Killian et al., 1990a). Upon interaction with interfacial environments, signal peptides adopt α-helical conformations [see, for instance, Briggs and Gierasch (1984) and Batenburg et al. (1988b)].

The tendency to adopt α-helical conformation is probably the best documented biophysical property of signal peptides, and has been demonstrated, in general, using circular dichroism

† This research was supported by a grant from the NIH to L.M.G. (GM-34962). J.R. and F.J.B. were fellows from the Ministerio de Educacion y Ciencia of Spain.

* Author to whom correspondence should be addressed.

‡ Department of Pharmacology.

§ Present address: Instituto de Estructura de la Materia, CSIC, Serrano 119, E-28006 Madrid, Spain.

‖ Department of Biochemistry.

⊥ Present address: Department of Chemistry and Biochemistry, University of Delaware, Newark, DE 19716.

0006-2960/93/0432-4881$04.00/0

(CD)[1] in membrane mimetic environments such as sodium dodecyl sulfate (SDS) micelles and phospholipid vesicles, or in bulk solvent mixtures that also mimic membrane environments, such as 2,2,2-trifluoroethanol (TFE)/water. CD techniques have been used to obtain information on overall contents of different types of regular secondary structure, but do not yield residue-specific information. To obtain more detailed information, we carried out conformational studies of signal peptides from the *Escherichia coli* outer membrane protein LamB in TFE-d_3/water mixtures using two-dimensional nuclear magnetic resonance (2D NMR) (Bruch et al., 1989; Bruch & Gierasch, 1990). These studies showed that the helix is most stable in the hydrophobic core and that the stability of the helix may be more important for biological activity than its length.

The work we present here was guided by two main goals. On one hand, we wanted to study another family of signal peptides by NMR in TFE-d_3/water to assess the generality of the results obtained on the LamB signal peptides. On the other hand, there are specific questions about the nature of the interactions between signal peptides and membranes that should be addressed using environments that are better mimics of biological membranes than TFE/water mixtures. For instance, is the conformation of signal peptides affected by electrostatic interactions between the positive charges at their N-terminus and the negatively charged membrane surface? Is there a strong association between the hydrophobic core and the hydrocarbon chains of the membranes? Are there conformational consequences from such association, and are there differences between peptides with differing biological activities? Hence, our second goal was to study in detail, using NMR, the conformations adopted by signal peptides in model membranes. Phospholipid vesicles are the ideal systems to address such questions, but the long correlation times associated with such systems hamper the application of conventional high-resolution NMR techniques. On the other hand, SDS micelles can be used as model membranes, and reasonable line widths have been observed for the NMR signals of a number of peptides interacting with SDS micelles (e.g., O'Neil & Sykes, 1989; Mammi & Peggion, 1990; Bairaktari et al., 1990a; Bruch et al., 1992).

In collaboration with Inouye and co-workers, we designed a series of mutants of the *E. coli* OmpA signal sequence to study the effect of changes in the length and hydrophobicity of the hydrophobic core on biological activity. Evaluation of the in vivo activity of these mutants (Lehnhardt et al., 1987; Goldstein et al., 1990, 1991; Tanji et al., 1991) and biophysical characterization of the isolated signal peptides (Hoyt & Gierasch, 1991a,b) have shown again that a high propensity for α-helix formation, and for insertion into phospholipid bilayers, characterizes the functional peptides. Here we present CD and NMR studies of the wild-type and several mutant OmpA signal peptides (Table I) in TFE/water and in SDS micelles. The analyses in the two conditions offer complementary information: the results obtained in TFE/water can be better related to intrinsic conformational properties of the peptides, while the experiments in SDS give information on the influence of the negatively charged surface of the micelles on these properties, and on the association of the peptides with the hydrophobic interior of the micelles. In TFE/water, we find that the helical conformation of the OmpA signal peptides starts right after the positively charged residues of the N-terminus and extends up to the C-terminus, in parallel with the results obtained for the LamB peptides. In SDS, a significant increase in the helicity of the N-terminus and the hydrophobic core is observed for the functional peptides. This increase in helicity is due to the interaction with the micelles and leads to a better correlation between helical content and functionality than that observed in TFE/water. In both environments, the helix is somewhat weaker between the hydrophobic core and the C-terminus, which may be a general property of signal sequences.

Table I: Peptides Studied

	peptide sequence[a]	export activity[b]
	1 5 10 15 20 22 25	
WT	M K K T A I A I A V A L A G F A T V A Q A / A P K D	●●●●
L6L8	L L	●●●●
Δ9	-	●●●●
Δ8	.	●●
Δ6-9	- - - -	○
18N	N	○

[a] The first four residues of the mature OmpA protein (APKD) have been included in all peptides to improve solubility; in addition, these four residues can avoid truncation effects in the behavior of the C–terminus of the signal sequence. The slash indicates the cleavage site of the signal peptidase. [b] In vivo activity as judged by the abilities of the wild-type and mutant signal sequences to mediate export of two heterologous proteins (Lehnhardt et al., 1987; Goldstein et al., 1990, 1991). Translocation of OmpA itself by several of these mutants is reported in Tanji et al. (1991). The relative activities do not change in the different systems.

EXPERIMENTAL PROCEDURES

The synthesis and purification of the peptides have been described previously (Hoyt & Gierasch, 1991a). All CD spectra were recorded on an AVIV Model 60DS spectropolarimeter equipped with a Hewlett-Packard 89100A temperature controller, following the same methods described in Bruch et al. (1989). To obtain estimates of secondary structure content by curve fitting to reference polylysine spectra (Greenfield & Fasman, 1969), we used an unrestrained least-squares-fit algorithm that optimizes the shape, rather than the absolute intensity, of the spectra. NMR spectra were recorded on a Varian VXR500 spectrometer at 500 MHz (proton frequency). Most spectra were acquired at 25 or 45 °C, on samples containing 2–2.5 mM peptide dissolved in TFE-d_3/H_2O 1:1 (v/v), with the apparent pH adjusted to 2.5 with dilute HCl, or in a 300 mM solution of SDS-d_{25} in dilute HCl with 10% D_2O (final pH 2.9). TFE-d_3 was 99.94% D from Cambridge Isotopes, and SDS-d_{25} was 99.4% D from MSD Isotopes. The residual signal from protonated TFE was used as reference [centered at 3.88 ppm downfield from 3-(trimethylsilyl)propionic acid] for the TFE-d_3/water samples. In the SDS-d_{25} samples, 3-(trimethylsilyl)propionic acid was used as internal reference. Two-dimensional total correlation spectroscopy (TOCSY) (Davis & Bax, 1985) and two-dimensional nuclear Overhauser effect spectroscopy (NOESY) (Jeener et al., 1979; Kumar et al., 1981) were used to obtain sequential resonance assignments (Wüthrich, 1986) and NOE patterns. Most parameters used for data acquisition and processing are analogous to those described in Bruch and Gierasch (1990). For NOESY and TOCSY spectra in TFE-d_3/water, the mixing times used were 300 and 75 ms, respectively; in SDS-d_{25}, they were 175 and 65 ms, respectively.

[1] Abbreviations: CD, circular dichroism; 1D, one dimensional; 2D, two dimensional; FID, free induction decay; NMR, nuclear magnetic resonance; NOE, nuclear Overhauser effect; NOESY, two-dimensional nuclear Overhauser effect spectroscopy; OmpA, outer membrane protein A; SDS, sodium dodecyl sulfate; TFE, 2,2,2-trifluoroethanol; TOCSY, two-dimensional total correlation spectroscopy.

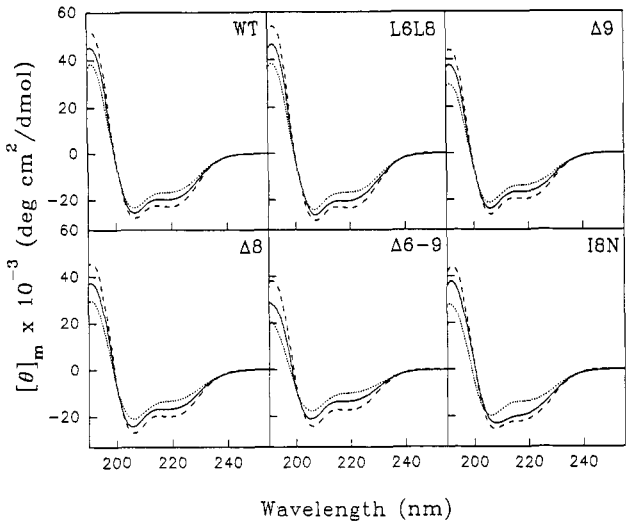

FIGURE 1: CD spectra of OmpA signal peptides in TFE/water 1:1 (v/v) at 5 °C (dashed line), 25 °C (solid line), and 45 °C (dotted line). Peptide concentrations were between 10 and 20 μM, and the apparent pH was 2.5.

Amide deuterium exchange rates were monitored by recording one-dimensional (1D) spectra at different times after the peptides were dissolved in a 300 mM solution of SDS-d_{25} in D_2O (Cambridge Isotopes, 99.996% deuteration) with a 2.9 final pD (uncorrected). To distinguish overlapping amide signals, we recorded a TOCSY spectrum after 90 min of exchange for both Δ6–9 and Δ8, and a NOESY spectrum for L6L8; the total acquisition time for these TOCSY and NOESY spectra was approximately 45 min (2 × 128 FIDs, 8 scans per FID). For the L6L8 peptide, we recorded additional NOESY spectra after 2 h 40 min and after 13 h 20 min of exchange, with total acquisition times of 90 min and 6.5 h, respectively.

RESULTS

Conformational Analysis in TFE/Water

Circular Dichroism. The CD spectrum of the WT OmpA signal peptide in aqueous solution reflects a predominantly random conformation (Hoyt & Gierasch, 1991a). In TFE/water 1:1 (v/v) at apparent pH 2.5, the CD spectrum of the WT peptide is characteristic of a highly α-helical conformation, with a double minimum at 208 and 222 nm (Figure 1). A TFE titration indicates that the conformational transition occurs mainly between 10% and 15% TFE (v/v), with the helical content increasing as the amount of TFE is raised, until a plateau is reached at concentrations of TFE higher than 30% (v/v) (data not shown). The CD spectrum in TFE/water 1:1 (v/v) at apparent pH 2.5 does not change significantly for WT peptide concentrations ranging from 10 μM to 1 mM, indicating no change in association state within this concentration range; at peptide concentrations around 10 μM, no changes in the CD spectrum are observed for a range of apparent pH values between 2.5 and 8.6. As could be expected, the spectrum at apparent pH 2.5 and 10 μM peptide concentration is temperature dependent, with decreasing amounts of helicity when the temperature is increased from 5 to 45 °C (Figure 1). The presence of an isodichroic point near 200 nm when the temperature is varied shows that the peptide is mainly visiting two conformational states. Indeed, curve fitting of the spectrum at 25 °C to reference polylysine spectra (Greenfield & Fasman, 1969) indicates that the peptide is 55–60% helical and 40–45% random, with a negligible contribution of β structure (Table II).

Table II: α-Helix Content and Helical Parameters *R*1 and *R*2 for OmpA Signal Peptides in TFE/Water[a]

peptide	% α-helix CD[b]	% α-helix NMR[c]	*R*1[d]	*R*2[e]
WT	55–60	58	−1.77	0.78
L6L8	60–65	52	−1.74	0.77
Δ9	50–55	51	−1.57	0.70
Δ8	50–55	51	−1.55	0.70
Δ6–9	40–50	40	−1.43	0.65
I8N	45–65[f]	54	−1.64	0.81

[a] All CD data collected in TFE/water 1:1 (v/v) at 25 °C, apparent pH 2.5, and 10–20 μM peptide concentrations. [b] Obtained by curve fitting to reference polylysine spectra (Greenfield & Fasman, 1969). The ranges of values given correspond to different percentages of α-helix calculated when the data were fit between 190 and 250 nm, or between 200 and 250 nm. The calculated percentage of β structure was zero in all peptides but I8N. [c] Calculated from Hα proton chemical shifts. The upfield shifts of Hα protons of residues in regions assumed to be helical were added, and an average conformational shift was calculated by dividing by the total number of peptide bonds. The average conformational shifts were divided by 0.35 ppm to obtain the α-helix percentages indicated (0.35 ppm is assumed to correspond to 100% α-helix; see text for further details). [d] *R*1 is defined as the ratio between the intensity of the maximum between 190 and 195 nm and the intensity of the minimum between 200 and 210 nm. [e] *R*2 is defined as the ratio between the intensity of the minimum near 222 nm and the intensity of the minimum between 200 and 210 nm. In some cases, a plateau, rather than a minimum, is observed near 222 nm; the average intensity in the plateau is used to calculate *R*2 in these cases. [f] The larger range of calculated helix percentage is due to the presence of some β structure (5–15%).

All the CD spectra of the peptides corresponding to mutant OmpA signal sequences in TFE/water 1:1 (v/v) are also indicative of helical structure (Figure 1). A two-state α-helix/random coil equilibrium also exists for most of the peptides, as is indicated by the isodichroic point observed in the CD spectra when the temperature is changed, and by the estimated contents of secondary structure (Table II). Only for the I8N mutant peptide is there some contribution of β structure to the conformational equilibrium (5–15% at 25 °C), which explains the lack of an isodichroic point for this peptide (Figure 1). These observations also correlate with the high tendency of the I8N peptide to aggregate when the temperature is raised (see below). In Table II are shown the estimates of helical content for each peptide obtained by curve fitting the CD spectra at 25 °C to reference polylysine spectra (Greenfield & Fasman, 1969). Although the helical contents calculated from $[\theta]_{222}$ correlated in relative terms with those obtained by curve fitting, they were difficult to reproduce, which is probably due to inaccuracies in the peptide concentrations obtained by amino acid analysis.[2] The curve-fitting method used is concentration independent and gave reproducible results. However, it is important to point out that small shifts in the wavelengths generated by the spectropolarimeter, especially in the 190–210-nm region, can produce large differences in the curve-fitting results when peptides have a high helical content. In addition, different results were obtained, in general, when data from 190 to 250 nm, or from 200 to 250 nm, were used in the fit (reflected as % helix ranges in Table II).

As independent parameters which could confirm whether the differences in the helical content of the peptides calculated

[2] This problem is particularly serious for hydrophobic peptides with a high tendency to aggregate. An interesting method to measure accurate peptide concentrations has been described by Baldwin and co-workers, who introduced a tyrosine residue in the N-terminus of designed model peptides to obtain concentrations from the aromatic absorbance at 275 nm (Marqusee et al., 1989).

Table III: Proton Chemical Shifts for OmpA Signal Peptides in TFE/Water[a]

	WT						L6L8		Δ9		Δ8		Δ6–9		I8N	
residue	NH	Hα	Hβ	Hγ	Hδ	other	NH	Hα	NH	Hα	NH	Hα	NH	Hα	NH	Hα
Met1		4.17	2.20	2.61		2.09		4.16		4.15		4.14		4.16		4.15
Lys2	8.52	4.45	1.90, 1.82	1.54, 1.48	1.72	3.01	8.50	4.46	8.49	4.45	8.49	4.44	8.52	4.44	8.54	4.43
Lys3	8.40	4.24	1.86, 1.81	1.52, 1.45	1.71	2.99	8.44	4.26	8.38	4.28	8.42	4.25	8.39	4.27	8.44	4.24
Thr4	7.63	4.17	4.22	1.26			7.65	4.19	7.67	4.24	7.68	4.24	7.73	4.21	7.69	4.22
Ala5	7.84	4.19	1.48				7.84	4.22	7.90	4.25	7.87	4.30	7.92	4.24	7.93	4.28
Ile6 (Leu)	7.48	3.89	1.89	1.57, 1.23, 0.94	0.89		7.57	4.17	7.50	3.93	7.51	3.94			7.58	3.96
Ala7	7.63	4.03	1.48				7.75	4.02	7.65	4.13	7.77	4.09			7.82	4.07
Ile8 (Leu,Asn)	7.65	3.79	1.92	1.69, 1.17, 0.93	0.84		7.61	4.17	7.52	3.87					7.88	4.50
Ala9	7.74	4.03	1.53				7.83	4.04			7.67	4.08			7.91	4.10
Val10	8.24	3.66	2.14	1.05, 0.93			8.11	3.67	7.56	3.69	7.58	3.74	7.54	3.86	8.08	3.67
Ala11	7.90	4.11	1.54				7.94	4.11	8.06	4.11	8.04	4.09	7.85	4.20	7.87	4.10
Leu12	8.56	4.23	1.90	1.60	0.88		8.54	4.24	8.02	4.24	8.13	4.24	7.79	4.28	7.98	4.23
Ala13	8.17	4.17	1.52				8.15	4.17	8.33	4.15	7.92	4.14	7.90	4.17	8.10	4.14
Gly14	8.21	3.92					8.23	3.89	8.22	3.88	8.21	3.87	8.13	3.86	8.25	3.85
		3.88						3.87				3.85				
Phe15	8.10	4.37	3.23			7.21	8.10	4.37	8.04	4.37	8.05	4.36	7.93	4.39	8.07	4.34
Ala16	8.45	4.01	1.52				8.47	4.03	8.50	4.02	8.45	4.01	8.29	4.07	8.51	4.00
Thr17	7.82	4.00	4.39	1.25			7.83	4.01	7.82	4.01	7.80	4.00	7.76	4.06	7.81	3.99
Val18	7.72	3.77	2.14	1.03, 0.93			7.73	3.77	7.70	3.77	7.70	3.76	7.66	3.82	7.71	3.75
Ala19	8.16	4.01	1.28				8.17	4.02	8.16	4.02	8.15	4.01	8.09	4.06	8.17	4.00
Gln20	7.70	4.16	2.19, 2.14	2.51, 2.39		7.19, 6.53	7.71	4.16	7.71	4.16	7.70	4.15	7.73	4.18	7.71	4.14
Ala21	7.72	4.31	1.44				7.73	4.31	7.73	4.30	7.72	4.29	7.74	4.31	7.72	4.29
Ala22	7.67	4.47	1.39				7.67	4.47	7.67	4.47	7.67	4.46	7.68	4.49	7.67	4.45
Pro23		4.41	2.29, 1.92	2.07, 2.02	3.80, 3.60			4.42		4.42		4.41		4.42		4.41
Lys24	8.10	4.42	1.92, 1.77	1.52	1.71	3.04	8.11	4.43	8.10	4.42	8.10	4.41	8.10	4.42	8.12	4.41
Asp25	8.01	4.72	2.93				8.01	4.72	8.00	4.73	8.00	4.73	8.01	4.74	8.01	

[a] All data were obtained in TFE-d_3/water 1:1 (v/v) at 25 °C, apparent pH 2.5, and peptide concentration 2–2.5 mM. Chemical shifts (in ppm) were referenced to the residual methylene resonance of TFE [centered 3.88 ppm downfield from 3-(trimethylsilyl)propionic acid]. The uncertainty is ±0.02 ppm. Note that an empty space has been left for the absent residues in the deletion mutants, so that the chemical shifts for homologous residues in all the peptides are in the same row. All the resonance assignments for the WT peptide are shown. Only the backbone proton assignments are indicated for the mutant peptides. For the side chains of the mutant peptides that are common to the WT peptide, most protons have very similar chemical shifts to those indicated (within 0.02 ppm), except for side chains neighboring the deleted or mutated residues, for which differences up to 0.06 ppm are observed. The assignments in the mutated residues are as follows: L6L8-Leu6, Hβ 1.76, Hγ 1.68, Hδ 0.93, 0.88; L6L8-Leu8, Hβ 1.76, Hγ 1.68, Hδ 0.93, 0.89; I8N-Asn8, Hβ 2.84, 2.80.

by curve fitting were significant, we used the $R1$ and $R2$ ratios described in Bruch et al. (1991) (see definition in Table II). These parameters are independent of peptide concentration and small wavelength shifts, and have been shown to be very useful in comparing relative helicity for closely related peptides when a two-state α-helix/random coil equilibrium exists (Bruch et al., 1991). For low helical content, $R1$ is positive, and $R2$ is close to zero. For highly helical peptides, $R1$ is close to −2, and $R2$ approaches 1. As can be observed in Table II, there is a good correlation between the $R1$ and $R2$ values calculated for each peptide and the helical content obtained by curve fitting, arguing that the differences in helicity among the peptides are significant. The highest uncertainty in the relative helical content corresponds to the I8N peptide, due to the presence of some amount of β structure. This peptide is the one that suffers the largest loss in helicity (about 15%) upon increasing the temperature from 25 to 45 °C, probably due to its tendency to aggregate. The helical content in all the other peptides decreases about 5–10% upon increasing the temperature to 45 °C, and increases about 5–10% when the temperature is lowered to 5 °C.

Nuclear Magnetic Resonance. Standard NMR methods were used to carry out sequential assignment of all the proton resonances of the six OmpA peptides in TFE-d_3/water 1:1 (v/v). TOCSY spectra were used to identify spin systems, and NOESY spectra were used to obtain interresidue connectivities and to distinguish equivalent spin systems. Although some clustering of cross-peaks occurred, in general, in the region between 4.0–4.2 and 7.6–7.8 ppm, unambiguous assignments could be obtained in all cases with the help of NH(i)/NH(i+1) and other NOE connectivities characteristic of helical conformation (see below). The assignments for all the protons in the wild-type peptide, and for the backbone protons of the mutant peptides, are shown in Table III. No major changes in the chemical shifts of the side chains were observed among homologous residues in the different peptides, and the maximum differences (0.05–0.06 ppm) occurred near the mutations or deletions. However, significant differences are observed in the backbone chemical shifts and are discussed below in terms of their correlation with conformational properties.

NOESY spectra with a 300-ms mixing time were recorded at 25 and 45 °C for all the peptides to obtain NOE patterns at both temperatures (no data could be obtained for I8N at 45 °C due to peptide aggregation). In these linear peptides, different mobilities are to be expected for different residues, and thus it is inappropriate to attempt a rigorous quantification of the NOEs. The relatively long mixing time used in the NOESY spectra (300 ms) was chosen to favor the observation of medium-range NOEs. The most significant interresidue NOEs observed at 25 °C, excluding Hα(i) or Hβ(i) to NH(i+1) interactions, are summarized in Figure 2. Several expansions of the NOESY spectra, where interactions characteristic of helical conformation have been labeled, are shown in Figure 3. Almost no Hα(i)/NH(i+2) NOEs were observed, which, together with the presence of Hα(i)/NH(i+4) interactions, shows that the peptides adopt α-helical rather than 3_{10}-helical conformation. The amide/amide and the fingerprint regions of the NOESY spectra of all the peptides contain more cross-peak overlap than the respective aliphatic regions, limiting the number of NH(i)/NH(i+2), Hα(i)/NH(i+3), and Hα(i)/NH(i+4) interactions that can be observed. As a result, the predominant medium-range NOEs that can be

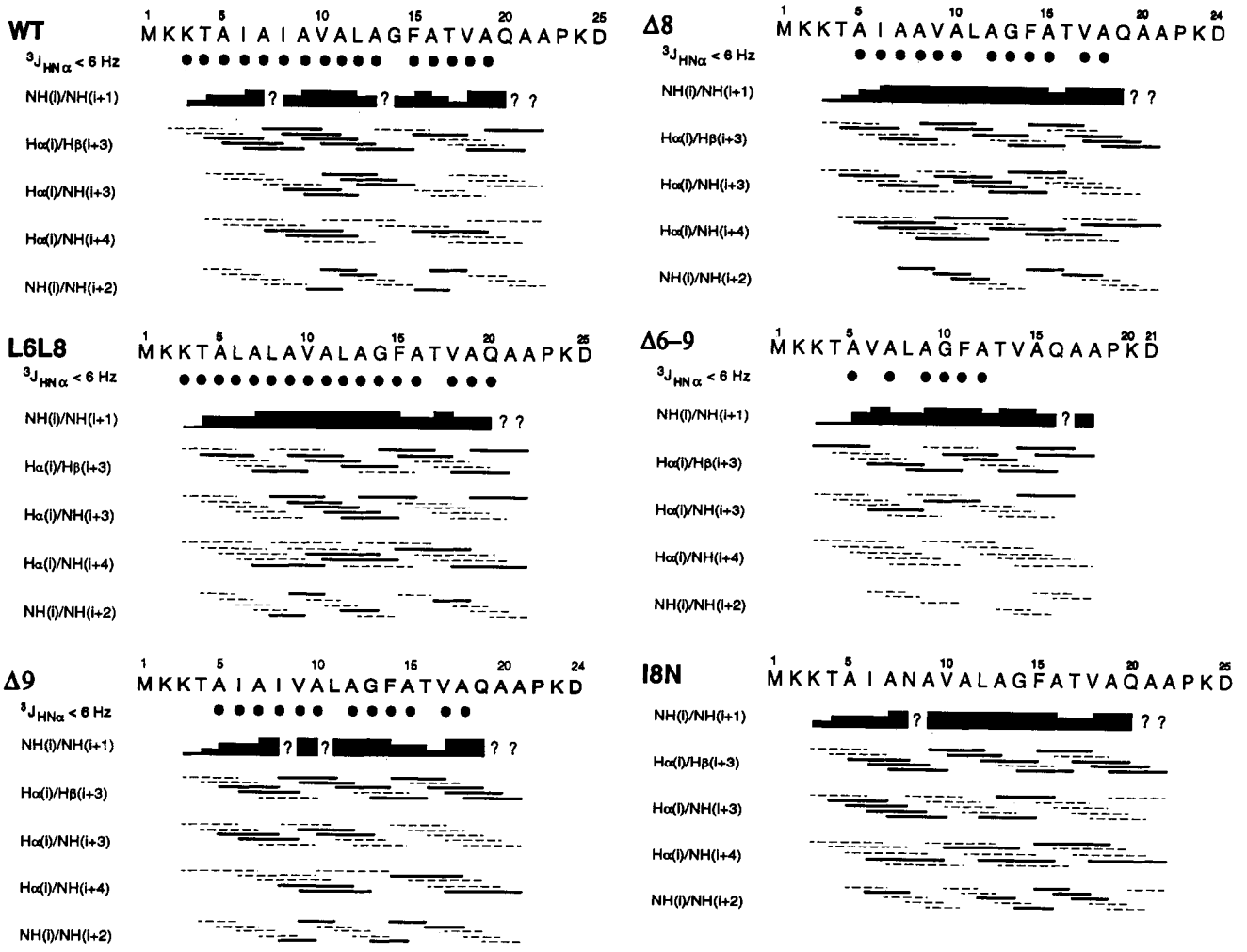

FIGURE 2: Summary of NOE data obtained for the OmpA signal peptides at 25 °C, with a mixing time of 300 ms. Only NH(i)/NH(i+1) and medium-range interactions are indicated. For the former, the height of the boxes is proportional to the estimated NOE intensities, and question marks indicate interactions that are too close to the diagonal to be assessed. Most medium-range interactions are weak, and their size is not reflected; solid bars indicate NOEs that have been identified, while dashed lines indicate NOEs whose presence or absence cannot be assessed due to overlap with intraresidue and sequential connectivities. $^3J_{HN\alpha}$ coupling constants that are smaller than 6 Hz at 45 °C are indicated with solid circles for all peptides except for I8N (which aggregates at 45 °C). For Gly residues, a solid circle indicates that both coupling constants are smaller than 6 Hz.

identified correspond to H$\alpha(i)$/H$\beta(i+3)$ interactions (Figure 2).

It is clear from the WT NOE pattern in Figure 2 that there are NOEs characteristic of α-helical structure throughout most of the wild-type OmpA peptide. The largest number of medium-range NOEs is observed in the hydrophobic core (residues 6–13), but several such NOEs are also observed up to the C-terminus of the signal sequence (Ala21). In the N-terminus, the helix is started at the Lys3 or Thr4 residues. The location of the helix appears to be very similar in the mutant peptides, as judged from their respective NOE patterns (Figure 2). When the NOE patterns of all the peptides are compared, it is clear that the lowest number of medium-range NOEs is observed in the deletion mutant Δ6–9, which is in agreement with the lower helicity observed for this peptide by CD. No substantial difference in the overall number of medium-range NOEs is observed between the other five peptides, although a detailed comparison is hindered by the overlap of cross-peaks.

As could be expected, the NOESY spectra recorded at 45 °C (data not shown) contain fewer and weaker medium-range NOEs, compared to the data obtained at 25 °C. The decrease in the number and intensity of such NOEs at the higher temperature originates both from a decrease in helical content and from an increase in overall motion (shorter correlation times). Overlap of resonances also hinders detailed comparison of the data for the different peptides, but the NOE patterns of most peptides indicate that the helix is fraying at the termini, particularly at the N-terminus, rather than weakening in the center. Only in the deletion mutant Δ6–9, for which almost no medium-range NOEs are observed at 45 °C, is there a loss of helicity throughout the sequence.

Additional conformational information on the OmpA signal peptides was obtained from backbone coupling constants. Small $^3J_{HN\alpha}$ coupling constants (<6 Hz) are expected for regions of polypeptides with high helical content, while values larger than 7 Hz are expected for residues that are mostly in an extended conformation (Wüthrich, 1986). Due to the substantial broadening of most NH resonances of the OmpA signal peptides in TFE-d_3/water at 25 °C, we measured values for the $^3J_{HN\alpha}$ coupling constants at 45 °C (no data could be obtained for I8N due to peptide aggregation) (Figure 2). For the WT peptide, most $^3J_{HN\alpha}$ values are smaller than 6 Hz from residues 3 to 19, which agrees with the localization of the helix deduced from the NOE data. Similar results are obtained for the L6L8 peptide, which according to the CD data has the same or higher helicity than the WT peptide (Table II). However, the coupling constants for residues 3

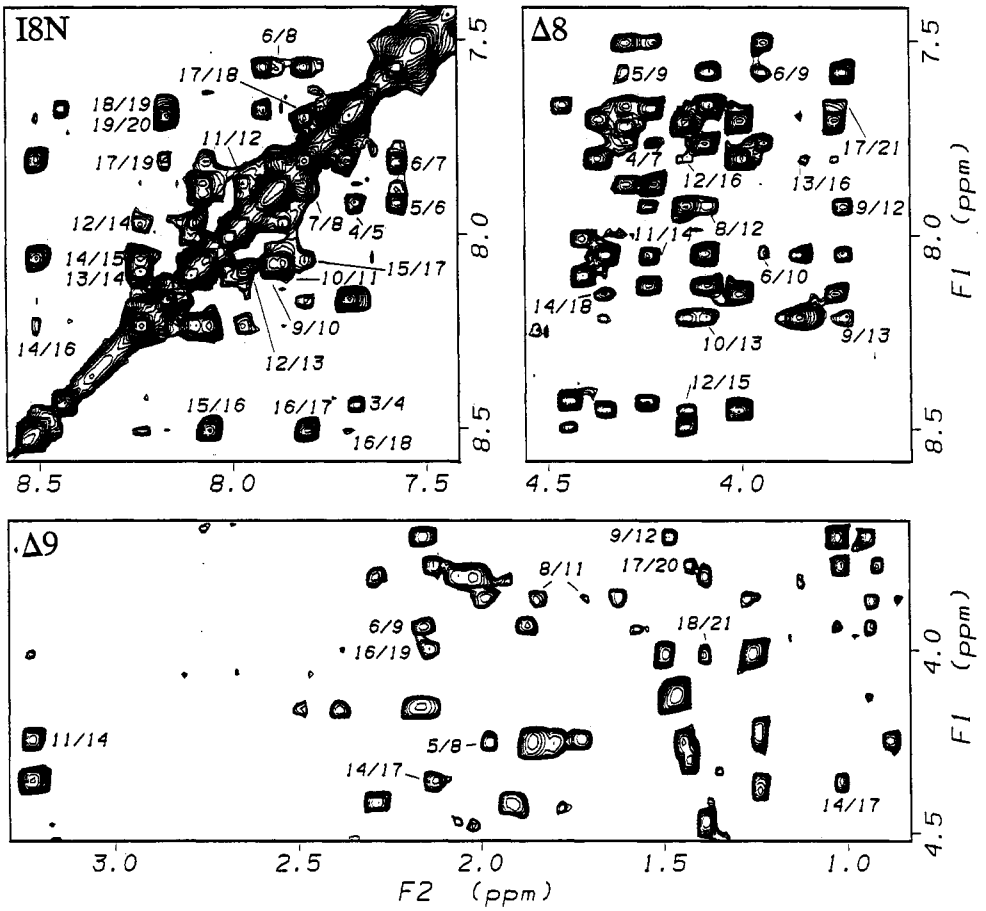

FIGURE 3: Contour plots corresponding to different regions of NOESY spectra of three OmpA peptides (obtained at 25 °C with a 300-ms mixing time). The data have been symmetrized for clarity. The residue numbers for each peptide correspond to those indicated in Figure 2. In the upper left corner is represented the amide/amide region of the NOESY spectrum of the I8N peptide, where NH(i)/NH(i+1) and NH(i)/NH(i+2) NOEs have been labeled. In the upper right corner is shown the fingerprint region of the NOESY spectrum of the Δ8 peptide, where the labeled cross-peaks correspond to Hα(i)/NH(i+3) and Hα(i)/NH(i+4) NOEs. Part of the aliphatic region of the NOESY spectrum of the Δ9 peptide, with labeled Hα(i)/Hβ(i+3) connectivities, is shown below.

and 4 in the Δ8 and Δ9 peptides are larger than 6 Hz, arguing that the lower helical content observed by CD in these two peptides may be due to some additional fraying of the helix in the N-terminus, compared to the WT and L6L8 peptides. The observation that only a few $^3J_{HN\alpha}$ coupling constants in the Δ6–9 peptide are small is indicative of lower helix content throughout the sequence, in agreement with the conclusions drawn from the NOE data.

Conformational Shifts. It has now been well established that the Hα protons of residues in an α-helical conformation experience an upfield shift with respect to random coil chemical shift values (Jiménez et al., 1987; Szilágyi & Jardetzky, 1989; Pastore & Saudek, 1990; Williamson, 1990; Wishart et al., 1991) and a chemical shift index based on Hα shifts has been proposed as a method to assign secondary structure in proteins (Wishart et al., 1992).[3] For peptides that are visiting exclusively random coil and α-helical conformations, with a rapid interconversion between both states, one can expect that the Hα proton of each residue will suffer an upfield shift proportional to the amount of time the residue spends in an α-helical conformation. Thus, the shifts of Hα protons (conformational shifts) can yield an approximate map of the relative percentage of helical structure adopted by each residue in the sequence. While a detailed comparison of the helicity of the OmpA peptides at the residue level using NOEs is hampered by cross-peak overlap problems and by quantitation difficulties, chemical shifts can be measured accurately and are not affected by the existence of different correlations times. Moreover, the average conformational shift can be used as an indicator of overall helical content. Hα chemical shifts have been used in a qualitative manner to analyze the conformation of short, linear peptides [see, for instance, Jimenez et al. (1987), Nelson and Kallenbach (1989), and Bruix et al. (1990)], but, to our knowledge, no attempt to use conformational shifts as helicity indexes in a semiquantitative way has been described.

Conformational shift maps for the OmpA peptides in TFE-d_3/water 1:1 at 25 °C (Figure 4) were obtained using as reference the random coil chemical shifts described in Wüthrich (1986). Although these reference shifts were obtained in water at pH 7.0 and 35 °C, they appear to be very insensitive to the conditions, as very small deviations (±0.02 ppm) were observed when several random coil Hα chemical shifts were measured in 30% TFE, at pH 5.4 and 22 °C (Jiménez et al., 1987). We also obtained overall helical content estimates (Table II) from average conformational shifts. To calculate such averages, only upfield shifts in the regions of the peptides assumed to be helical (these include residues 3 to the Ala in the C-terminus of the signal sequence) were considered. A zero contribution was assigned to the small upfield and downfield shifts occurring at the termini, which were considered as nonhelical. Lacking stereospecific assign-

[3] The dependence of the chemical shift of Hα protons on the secondary structure of polypeptides can be correlated with the distance between these protons and nearby oxygen atoms from carbonyl groups in each type of secondary structure (Pardi et al., 1983).

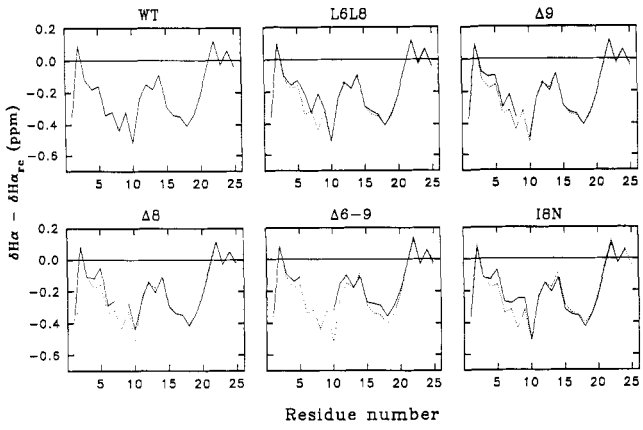

FIGURE 4: Conformational shift maps for the six OmpA peptides in TFE-d_3/water 1:1 (v/v) at 25 °C. The differences between the observed Hα proton chemical shifts and the random coil values described in Wüthrich (1986) are represented as a function of the residue number for each peptide (solid lines). In the plots corresponding to mutant peptides, the profile corresponding to the WT peptide has been represented by a dashed line. An empty space has been left for deleted residues to facilitate comparison between the deletion mutants and the WT peptide.

ments for the Gly Hα protons, and assuming that the Gly residue is at least partially involved in helix formation, we used the larger upfield shift to compute the average. Thus, an average conformational shift was calculated for each peptide by adding all upfield shifts in helical regions and dividing by the total number of peptide bonds. To obtain overall helical contents for each peptide, we divided the average conformational shifts by 0.35 ppm, which we assigned as an average for 100% helicity. The 0.35 ppm shift was taken as a compromise among several values that have been described for the average upfield shift observed in proteins for Hα protons of residues in an α-helical conformation: 0.3 ppm (Williamson, 1990), 0.35 ppm (Jiménez et al., 1987), 0.39 ppm (Wishart et al., 1991), and 0.4 ppm (Szilágyi & Jardetzky, 1989).

The agreement between the α-helical contents calculated from the CD data and from the conformational shifts (Table II) is remarkably good. This correlation argues that the approximations made are reasonable enough to justify the use of average conformational shifts to obtain estimates of overall helical content. A caveat of the method is that the side chain of each residue can also influence the observed upfield shifts. This is reflected in the difference in helicity calculated for the WT and L6L8 peptides, which appear to have very similar helical content according to the CD data. The difference originates in the double Ile → Leu substitution, as large upfield shifts are observed systematically for the β-branched residues Ile and Val. This observation correlates with statistical data obtained for proteins, which indicate that Ile and Val Hα protons experience the largest upfield shifts when these residues adopt helical conformations (Wishart et al., 1991). The accuracy of the analysis of helical content using Hα chemical shifts will improve when reference values of α-helical upfield shifts for each type of residue are introduced in the calculations.

The conformational shift maps shown in Figure 4 are very useful to analyze the location of the α-helical regions in the OmpA peptides and make comparisons among them. The upfield shifts observed for the WT peptide (Figure 4) indicate that the helix starts at Lys3 and extends to Ala20, in agreement with the conclusions deduced from the other NMR parameters. At the N-terminus, the helicity appears to increase progressively, with residues 3–5 only partially helical and the hydrophobic core forming a stable helix. At the C-terminus, the helix appears to end more abruptly, perhaps because of the helix-destabilizing proline residue. In addition, the conformational shifts clearly show that some weakening of the helix occurs around Gly14, which could be expected given the low helix propensity of Gly residues (Chakrabartty et al., 1991). This feature is common to all of the peptides, but was not apparent from the analysis of NOE patterns and coupling constants (Figure 2). The conformational shift profile of the L6L8 peptide (Figure 4) is almost identical to that of the WT peptide (the only differences correspond to the Ile → Leu mutations), arguing that the distribution of the helix along both peptides is very similar. For the Δ9, Δ8, and I8N mutants, the upfield shifts are almost identical to the WT peptide from residue 10 to the C-terminus, but they are slightly smaller in the N-terminus, including a good part of the hydrophobic core (Figure 4). These observations clearly show that the lower helical content of these peptides compared to the WT peptide is due to additional fraying of the helix in the N-terminal region, as was suggested by the coupling constants obtained for Δ9 and Δ8. The conformational shifts also confirm that the loss of helicity in the Δ6–9 peptide occurs through most of the sequence (Figure 4).

Our NMR study of LamB signal peptides suggested that the stability of the helix in the hydrophobic core could be more important for biological activity than the length of the helix (Bruch & Gierasch, 1990). In order to gain further insight into the stability of the helix in different regions of the OmpA peptides, we compared the conformational shifts at 25 °C with those at 45 °C (data not shown). The helix percentage calculated from the average upfield shifts decreased only 2–3% in the WT and L6L8 peptides, and 6–9% in Δ9, Δ8, and Δ6–9. For the WT and L6L8 peptides, the conformational shifts at 45 °C are almost identical to those at 25 °C from residues 8 to 14, and some decrease in helicity is observed at both termini. In Δ9, Δ8, and Δ6–9, the major helix destabilization occurs also at the termini, but some decrease in helicity is observed in the central region of the peptides. Thus, for the OmpA peptides in the conditions of this study, it appears that a relatively stable helix in the hydrophobic core is a property of two functional peptides, WT and L6L8, but the distinction between functional and nonfunctional peptides is not clear-cut.

Analysis in SDS Micelles

One-Dimensional NMR Spectra. Our previous work with synthetic OmpA signal peptides showed that they have a high tendency to aggregate in aqueous solution (Hoyt et al., 1991a). These studies also showed that low pH (less than 3) was necessary to keep the WT peptide in aqueous solution for prolonged periods of time (more than 15 h) at 100 μM peptide concentration. Nonetheless, attempts to maintain the WT peptide in solution at millimolar concentrations with SDS-d_{25} concentrations up to 300 mM, and temperatures up to 45 °C, were unsuccessful. As our previous experience indicated that the L6L8 peptide, which has wild-type in vivo activity, is less prone to aggregation, we attempted to dissolve this peptide at 2 mM concentration in 300 mM SDS-d_{25}, at pH 2.9 and 25 °C. Although broad lines were observed in the 1D NMR spectrum (see Figure 5), no sign of aggregation was observed for several days, which allowed us to record two-dimensional NMR data. We were also able to obtain NMR spectra in the same conditions for the kinetically defective Δ8 mutant, and the export-defective mutant, Δ6–9. Despite the occurrence of some aggregation, a time-independent NMR spectrum was also observed for the functional Δ9 peptide. The export-

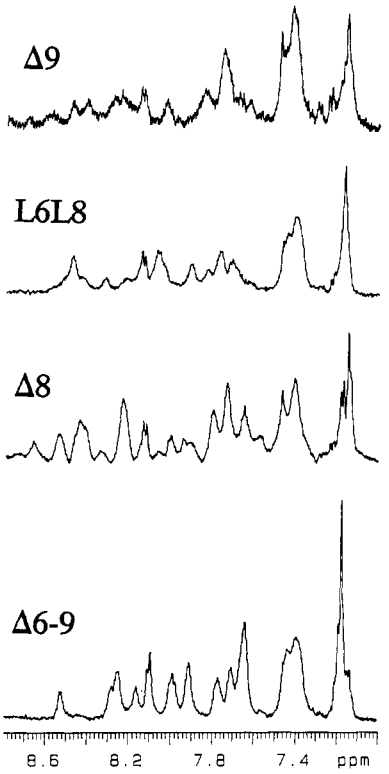

FIGURE 5: Amide/aromatic region of the 500-MHz ^{1}H NMR spectra of four OmpA peptides in 300 mM SDS-d_{25} (10% D_2O, pH 2.9) at 25 °C. All spectra are the result of 128 scans, with a 6000-Hz spectral width; 16 000 complex points were acquired in each case, and 0.2-Hz line broadening was applied before Fourier transformation. All spectra have been plotted to the same scale, except for that corresponding to Δ9, which has been plotted with a vertical scale 3 times larger.

defective I8N peptide displayed an even higher tendency to aggregate than did the WT peptide.

The low-field regions of the ^{1}H NMR spectra of the four OmpA peptides in 300 mM SDS-d_{25} are compared in Figure 5. The interaction with the micelles causes broadening of the NMR signals for all the peptides, but the extent of this broadening differs substantially among the peptides. The broader lines are observed for the Δ9 and L6L8 peptides, while relatively sharp lines can still be observed for Δ6–9. These observations indicate that the peptides corresponding to functional signal sequences associate more strongly with the micelles than does the export-defective mutant Δ6–9; the degree of association of the kinetically defective mutant, Δ8, appears to be intermediate between the functional and nonfunctional peptides.

NOE Analysis. In order to assign the ^{1}H NMR spectra of the OmpA peptides in 300 mM SDS-d_{25} micelles at 25 °C, we also applied the sequential assignment method (Wüthrich, 1986) using TOCSY and NOESY spectra. No major problems were encountered in the assignment of the Δ6–9 and Δ8 peptides, which was facilitated by the good quality of the two-dimensional data obtained. Assignment of the L6L8 peptide was considerably more difficult, in particular because of the poor quality of the TOCSY data. However, combining information obtained at 25 and 45 °C, and also with the help of medium-range NOEs, we were able to assign all the proton resonances of the L6L8 peptide. For the Δ9 peptide, which experienced partial aggregation, we were not able to complete all the assignments due to the poor quality of both the TOCSY and the NOESY data. However, combining data obtained at 25 and 45 °C in SDS-d_{25}/H_2O and in SDS-d_{25}/D_2O solutions, we were able to obtain assignments for all the Hα protons to calculate conformational shifts. In Table IV are summarized the assignments corresponding to the backbone protons of L6L8, Δ6–9, and Δ8, as well as those for the Hα protons of Δ9. No major differences were found between the chemical shifts of the side chain protons of the OmpA peptides in SDS micelles and those observed in TFE-d_3/water 1:1.

The amide/amide and medium-range NOEs observed for the L6L8, Δ8, and Δ6–9 peptides are summarized in Figure 6. The NOE patterns for the three peptides are strongly indicative of a helical conformation extending throughout most of the signal sequence. As observed in the TFE/water data, the largest number of medium-range interactions can be found in the aliphatic region of the NOESY spectra (represented for L6L8 and Δ6–9 in Figure 7), as it has less cross-peak overlap than the fingerprint and the amide/amide regions. A detailed comparison among the peptides is also hindered here by the cross-peak overlap problem and by difficulties in NOE quantitation. The quantitation problem is exacerbated here because it can be expected that different parts of the peptides would experience a different degree of partitioning between an aqueous environment, where the peptides adopt mainly random conformation, and the micelles, which induce the formation of α-helical structure. As much longer correlation times can be expected in the micellar environment, the NOE patterns will be weighted in favor of the conformations induced by the interaction with the micelles. This point is illustrated, for instance, in the NOE pattern observed for the Δ6–9 peptide (Figure 6): although the α-helix content of this peptide in the conditions of the study is only 50% (see below), the NOE pattern suggests that most of the peptide is helical. When compared with the pattern observed for the L6L8 peptide (Figure 6), no clear difference in the number of medium-range interactions can be observed, even though there is a substantial difference in helical content among the two peptides (see below). No significant differences are apparent either when the intensities of the medium-range interactions in the two peptides are compared.

The NOE overlap and quantitation problems also hinder a detailed comparison between the conformations of the peptides in SDS micelles and those observed in TFE/water. However, an analogy and a distinction can be made when the NOE patterns observed in both environments are compared. The helical region of all the peptides appears to extend up to the C-terminal end of the signal sequence (Ala21 in the wild-type sequence) both in TFE/water and in SDS micelles. On the other hand, the helix appears to be more extended toward the N-terminus in the micellar environment than in TFE/water, as indicated by Lys2 NH/Lys3 NH NOEs for all peptides in SDS (not observed in TFE/water) and by the larger intensity of the other N-terminal amide/amide NOEs observed in SDS. The extension of the helix toward the N-terminus is also supported by analysis of the upfield shifts of Hα protons and by amide deuterium exchange rates (see below).

Conformational Shifts. In Figure 8 are shown the conformational shift maps for the L6L8, Δ9, Δ8, and Δ6–9 OmpA peptides in SDS micelles, compared with the maps obtained in TFE/water. The similarities between the conformational shifts obtained in TFE/water and in SDS for the C-terminal residues in each peptide argue that the conformational behavior of the C-terminus of each peptide in either milieu is very similar. On the other hand, the conformational shift map observed for the functional L6L8 peptide in SDS shows that the helicity of the hydrophobic core, and especially of the

Table IV: Backbone Proton Chemical Shifts for OmpA Signal Peptides in SDS Micelles[a]

	L6L8		Δ8		Δ6–9		Δ9
	NH	Hα	NH	Hα	NH	Hα	Hα
Met1		4.24		4.22		4.20	4.26
Lys2	8.48	4.39	8.47	4.49	8.54	4.38	4.46
Lys3	8.32	4.12	8.44	4.07	8.30	4.19	4.06
Thr4	7.77	3.95	7.74	4.04	7.79	4.08	3.92
Ala5	7.62	4.04	7.57	4.29	7.73	4.21	4.11
Ile6 (Leu)	7.69	4.04	7.65	3.73			3.73
Ala7	7.91	3.98	7.95	3.94			4.00
Ile8 (Leu)	7.91	4.02					3.68
Ala9	8.04	3.96	7.74	4.07			
Val10	8.09	3.56	7.74	3.77	7.68	3.81	3.65
Ala11	8.07	4.01	8.24	3.99	7.93	4.19	4.01
Leu12	8.47	4.10	8.41	4.09	8.02	4.16	4.10
Ala13	8.22	4.07	7.81	4.22	7.92	4.17	4.12
Gly14	8.52	3.80	8.55	3.88	8.26	3.91	3.80
		3.70		3.67		3.77	
Phe15	8.51	4.32	8.66	4.23	8.26	4.33	4.29
Ala16	8.43	3.98	8.22	4.02	8.17	4.05	3.99
Thr17	7.83	4.01	7.80	3.98	7.78	4.03	4.00
Val18	7.83	3.81	7.81	3.75	7.67	3.80	3.76
Ala19	8.16	4.03	8.25	3.98	8.11	4.02	4.01
Gln20	7.79	4.17	7.64	4.16	7.73	4.16	4.18
Ala21	7.72	4.28	7.66	4.29	7.66	4.29	4.30
Ala22	7.76	4.45	7.73	4.41	7.66	4.42	4.45
Pro23		4.41		4.42		4.41	4.44
Lys24	8.06	4.33	8.02	4.35	8.00	4.35	4.36
Asp25	8.14	4.73	8.14		8.12		

[a] Data obtained in 300 mM SDS-d_{25} at pH 2.9 and 25 °C. Chemical shifts (in ppm) were referenced to 3-(trimethylsilyl)propionic acid. The uncertainty is ±0.02 ppm. An empty space has been left for the absent residues in the deletion mutants in order to have the chemical shifts for homologous residues in all the peptides in the same row. Only Hα proton assignments are indicated for Δ9.

N-terminus, increases considerably with respect to that observed in TFE/water. Interestingly, similar conclusions can be drawn for the functional Δ9 peptide, while only a slight increase in the helicity of a few residues is observed for the export-defective Δ6–9 mutant. The conformational shift map for the kinetically defective Δ8 peptide in SDS indicates an increase in helicity in the hydrophobic core and in the N-terminus with respect to the profile observed in TFE/water, but the increase is less marked than in L6L8 and Δ9. Hence, the behavior of the Δ8 peptide is again intermediate between the functional and nonfunctional peptides.

The analysis of the conformational shifts corroborates and refines the conclusion, drawn from the NOE data, that an increased helicity in the N-terminal region is observed when the conformations of the OmpA peptides in SDS micelles are compared to those found in TFE/water. To obtain a semiquantitative measure of the overall increase in helicity, we calculated helix contents for each peptide from the average upfield shift of the Hα protons as described above (Table V). The helix contents calculated with this method for the L6L8 and Δ9 peptides in SDS are about 20% larger than those obtained in TFE/water (Table II), while more modest increases in helicity are observed for Δ8 and Δ6–9 (15% and 10%, respectively). Hence, the functional peptides experience a larger increase in helix content, as was deduced from qualitative examination of the conformational shift maps. Most important, there is a clear correlation between the helix content of the OmpA peptides in SDS micelles and their in vivo activity.

Amide Deuterium Exchange Rates. To study the degree of protection of the amide protons from the solvent, we dissolved samples of the L6L8, Δ8, and Δ6–9 OmpA peptides in 300 mM SDS-d_{25}/D_2O (pD 2.9 uncorrected, 25 °C) and monitored the disappearance with time of the amide resonances in 1D NMR spectra. The results are summarized in Figure 9. A large difference in the deuterium exchange rates of the amide protons in the hydrophobic core can be observed between the L6L8 peptide and the Δ8 and Δ6–9 mutants. Some amide protons remain protonated after 54 h of exchange in L6L8, arguing that a stable helix is formed (Rohl et al., 1992; Henry & Sykes, 1990). Protection by the hydrophobic chains of the detergent probably also contributes to the slow exchange rates. Exchange at both ends of the signal sequence is also somewhat slower in L6L8 than in Δ8 and Δ6–9. Hence, the stabilization of the helix produced in the hydrophobic core of the functional peptide by interaction with the micelles propagates to a certain extent toward both the N- and C-termini. However, a short stretch of residues between the hydrophobic core and the C-terminus (around Gly14) has relatively more exposed amides, suggesting that the helix is bent or is less stable in this region. Such weakening of the helix was also present in TFE-d_3/water, although the conformational shifts indicate that it is less pronounced in SDS micelles (Figure 8). At the N-terminus, there is some degree of protection even in the amide proton of Lys2, while the first protected amide proton observed for the L6L8 peptide in TFE-d_3/D_2O corresponds to Leu6 (data not shown). This observation is consistent with the conclusion from conformational shifts that the N-terminus is more helical in SDS than in TFE/water, but cannot be explained from hydrogen bonding, as the first three amide protons of an α-helix are not expected to be intramolecularly hydrogen bonded. Instead, these data support some protection from interaction with the micelle.

Analysis of CD Spectra. The estimates of α-helix content in SDS micelles calculated for the L6L8, Δ9, Δ8, and Δ6–9 OmpA peptides from the average conformational shifts (Table V) indicate that there is a correlation for these peptides between helicity in SDS and biological activity. However, this correlation was less clear when the α-helix percentages obtained by circular dichroism from the mean residue ellipticity at 222 nm were considered (Hoyt & Gierasch, 1991a). When these helix contents are compared with those calculated from the conformational shifts (Table V), significant discrepancies

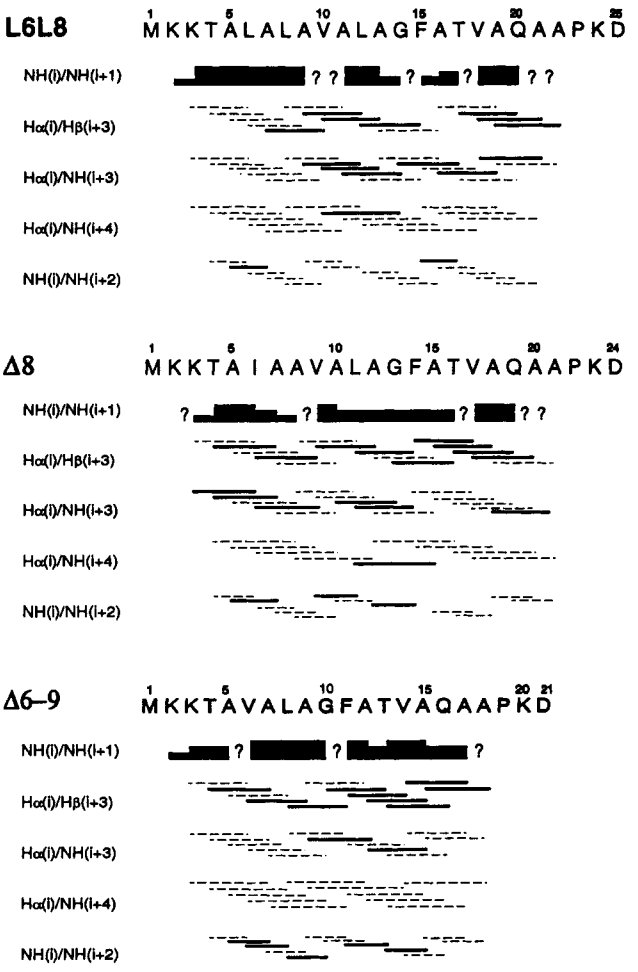

FIGURE 6: Summary of the conformationally most relevant NOEs observed for the L6L8, Δ8, and Δ6–9 OmpA peptides in 300 mM SDS-d_{25} at pH 2.9 and 25 °C (175-ms mixing time). For the NH-(i)/NH(i+1) NOEs, the estimated intensities are reflected by the height of the boxes, and question marks indicate interactions that could not be assessed because of overlap with the diagonal. No quantification is indicated for the medium-range NOEs, which are indicated by solid bars. Medium-range interactions whose presence could not be assessed due to overlap with intraresidue or sequential NOEs are represented by dashed lines.

are observed in the values obtained for Δ9 and Δ6–9. As mentioned above, we had difficulties in obtaining reproducible helix contents in TFE/water from $[\theta]_{222}$ due to inaccuracies in peptide concentrations. Hence, we decided to reanalyze the CD data on the OmpA peptides in SDS micelles described in Hoyt and Gierasch (1991a) using methods that are independent of the peptide concentration.

Curve fitting to reference polylysine spectra (Greenfield & Fasman, 1969) yielded results significantly different from those obtained from $[\theta]_{222}$ for several peptides (Table V). Interestingly, the curve-fitting results for the four peptides that could be studied by NMR show a very good agreement with the helix contents calculated from the conformational shifts. We also calculated, from the CD data of the OmpA peptides in SDS, values for the parameters $R1$ and $R2$ described above. A good correlation is observed between the values of $R1$ and the curve-fitting results (Table V). Note also that the values of $R1$ obtained for the functional peptides in SDS are more negative than those obtained in TFE/water (Table II), in accordance with the conclusion that these peptides are more helical in SDS. $R2$ also correlates with the curve-fitting and NMR results (Table V), but is less sensitive to helix content for highly helical peptides such as the functional OmpA peptides in SDS.

DISCUSSION

Our goals in this work were to study the conformational behavior of the OmpA signal peptides in two different environments, TFE/water and SDS micelles, and to establish comparisons among the peptides that could lead to insights into their biological function. Hence, in addition to using standard methods of analysis of CD and NMR results, we have put particular emphasis on parameters that are not so widely used but are very helpful to compare peptides with very similar sequence. This methodology also facilitates the analysis of OmpA peptides in SDS micelles and the comparison of results obtained in the two environments. In our CD analysis, the $R1$ and $R2$ parameters were very useful to compare the helical tendencies of the peptides due to their reproducibility, independently of small wavelength shifts and errors in peptide concentrations. In the NMR analysis, the conformational shifts were extremely useful to study the helicity of the peptides at the residue level, allowed a more detailed comparison among the peptides than the NOE data, and enabled us to compare the conformational behavior of Δ9 in SDS miceles with that of L6L8, Δ8, and Δ6–9, despite our inability to obtain complete assignments and NOE patterns for the former peptide. In addition, the conformational shifts yielded estimates of overall helical content that correlate reasonably well with the CD data. With no doubt, the reliability of helix quantitation methods based on conformational shifts will improve with the inclusion of reference upfield shifts for each residue type.

Analysis in TFE/Water. TFE appears to be a strong agent for helix induction in polypeptides, but only in those regions with some tendency for helicity (Dyson et al., 1988; Nelson & Kallenbach, 1989). Hence, the study of OmpA signal peptides in TFE/water allows us to analyze their intrinsic helical propensities. The WT OmpA signal peptide has the ability to adopt substantial amounts of α-helical conformation, a property that has been observed in all signal peptides studied so far. As was observed in the LamB signal peptide (Bruch et al., 1989; Bruch & Gierasch, 1990), the helix starts right after the positive charges at the N-terminus and is most stable in the hydrophobic core. A double Ile → Leu substitution did not affect function and was not expected to change substantially the conformational behavior of the signal sequence; in agreement with this prediction, the amount and distribution of helicity in the L6L8 peptide are almost identical to WT. The lower helicity in the other functional peptide studied, Δ9, can also be rationalized from the conformational point of view, as the deletion in position 9 removes a residue with high helix propensity, Ala, and shortens the length of the hydrophobic core. However, the kinetically defective mutant, Δ8, has a very similar behavior to Δ9, despite the fact that the residue removed in the hydrophobic core, Ile, has a lower potential to form helix than Ala (Padmanabhan et al., 1990; O'Neil & DeGrado, 1990). Hence, it appears that shortening of the hydrophobic core is the major determinant for the loss of helicity in both Δ8 and Δ9. Consistent with this observation, deletion of four residues in the hydrophobic core (Δ6–9 mutant) results in a major decrease in helical content that affects the whole sequence, as it did in the Δ78 LamB mutant (Bruch & Gierasch, 1990). In the LamB Δ78 mutant, the four-residue deletion brings into proximity two helix-breaking residues, Pro and Gly, which helped explain the loss in helicity. Although there is no proline in the N-terminus of the OmpA signal sequence, deletion of residues in the hydrophobic core results in an approach between the N-terminal positive charges, which oppose helix formation due to unfavorable electrostatic

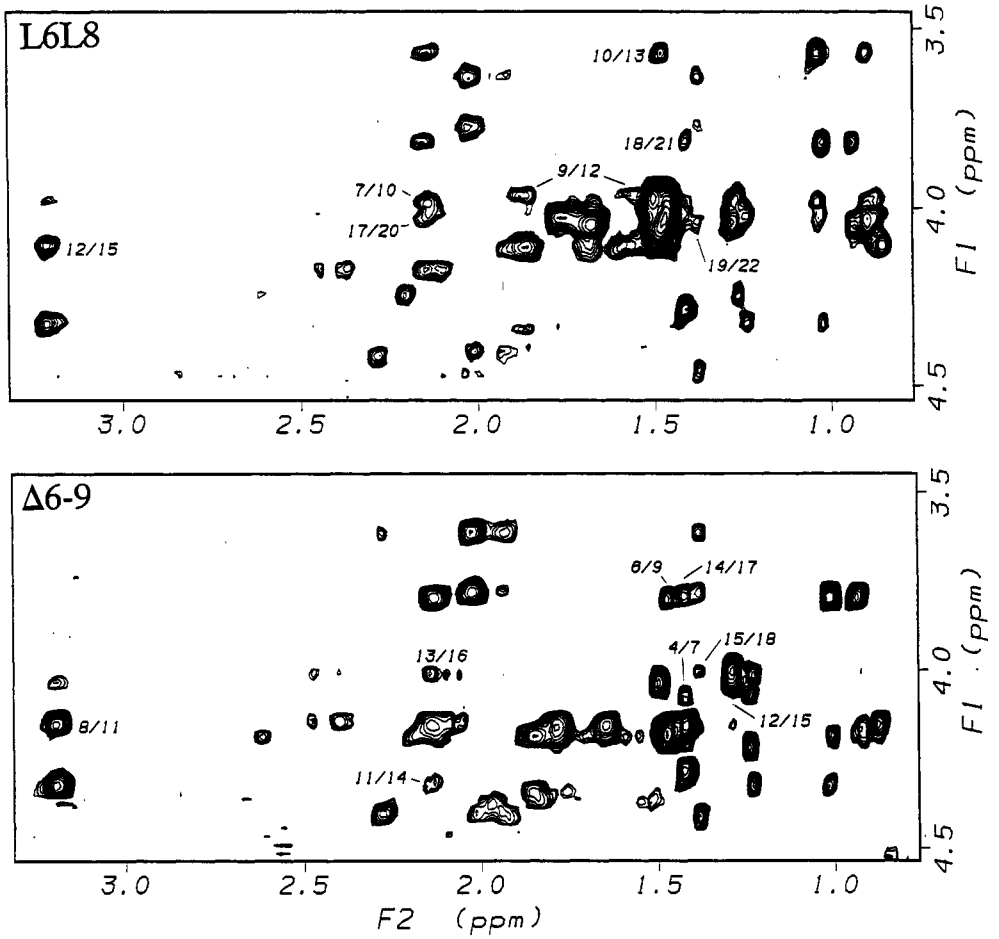

FIGURE 7: Contour plots corresponding to the aliphatic region of the NOESY spectra of the L6L8 and Δ6–9 OmpA peptides in 300 mM SDS-d_{25} at 25 °C (175-ms mixing time). The data have been symmetrized for clarity. The labeled cross-peaks correspond to Hα(i)/Hβ(i+3) NOEs. Residue numbers correspond to those indicated in Figure 6.

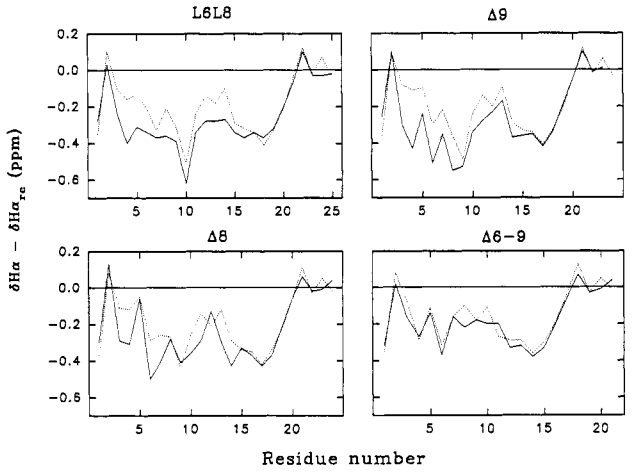

FIGURE 8: Conformational shift maps for the L6L8, Δ9, Δ8, and Δ6–9 OmpA peptides in 300 mM SDS-d_{25} at 25 °C (solid lines). The difference between the Hα chemical shifts observed and the random coil chemical shifts described in Wüthrich (1986) is represented as a function of the residue number for each peptide. For comparison purposes, the conformational shifts observed in TFE-d_3/water 1:1 (v/v) are also represented (dashed lines).

Table V: α-Helix Content and Helical Parameters $R1$ and $R2$ for OmpA Signal Peptides in SDS Micelles[a]

peptide	% α-helix			$R1$[e]	$R2$[e]
	$[\theta]_{222}$[b]	curve fitting[c]	NMR[d]		
WT	64	65–70		−2.03	0.83
L6L8	60	60–70	71	−1.86	0.79
Δ9	50	65–70	72	−1.84	0.76
Δ8	60	60–65	66	−1.75	0.77
Δ6–9	24	50–55	50	−1.38	0.62
I8N	44	55–60		−1.50	0.65

[a] The CD helical contents and the $R1$ and $R2$ parameters have been calculated from our previously published CD spectra, which were obtained in 40 mM SDS at 25 °C and 5 μM peptide concentration (Hoyt & Gierasch, 1991a). NMR data were acquired in 300 mM SDS-d_{25} at 25 °C and 2 mM peptide concentration. [b] Data from Hoyt and Gierasch (1991a), calculated from $[\theta]_{222}$ according to the method of Chen et al. (1974). [c] Obtained by curve fitting to reference polylysine spectra (Greenfield & Fasman, 1969). The ranges of values given correspond to different percentages of α-helix calculated when the data were fit between 190 and 250 nm, or between 200 and 250 nm. The calculated percentage of β structure was zero in all cases. [d] Calculated from Hα proton chemical shifts using the method described in the text and in Table II. [e] $R1$ and $R2$ are defined in Table II.

interactions with the helix dipole, and the glycine residue. The other functionally defective peptide studied, I8N, incorporates Asn, a residue with a tendency to hydrogen bond with the backbone and disrupt α-helices, in the center of the hydrophobic core; the result of this substitution is a modest loss of helicity in the hydrophobic core that extends toward the N-terminus in a similar manner to that observed in Δ8 and Δ9.

The conformational shift maps of the OmpA peptides in TFE-d_3/water (Figure 4) show that a short region at the C-terminus of the hydrophobic core has low helicity, and one may ask if this feature has functional importance. Construction of a conformational shift map for the LamB signal peptide using the assignments described in Bruch et al. (1989)

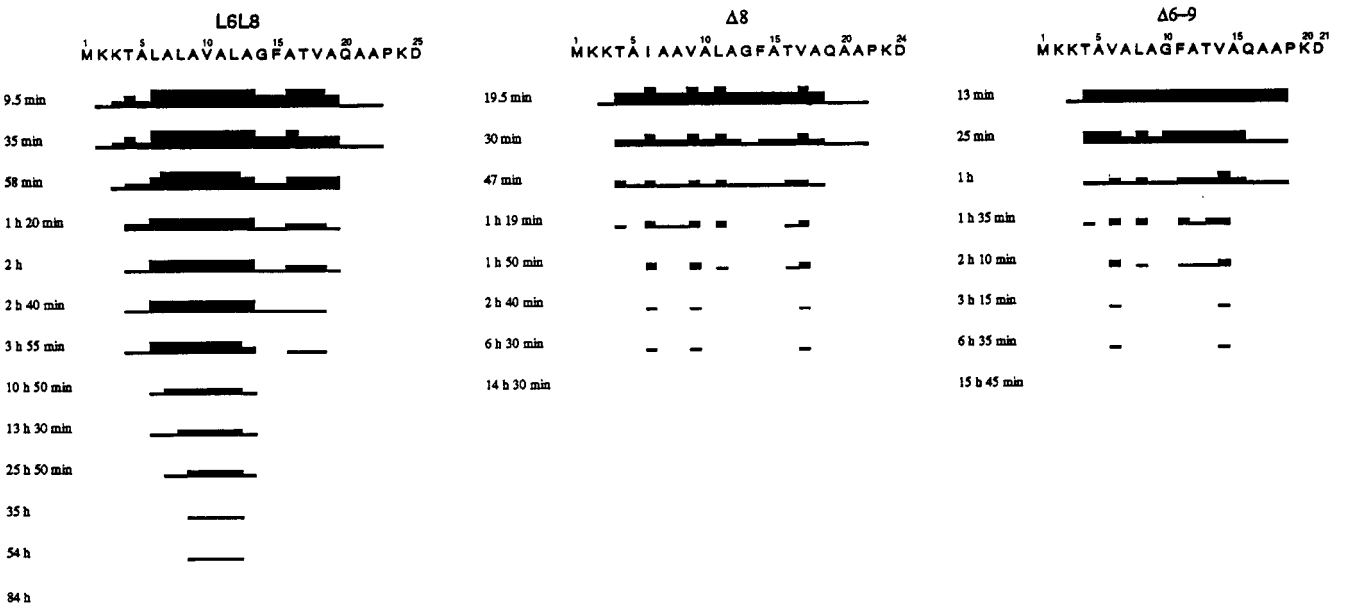

FIGURE 9: Summary of the evolution of the amide deuterium exchange experiments performed for the L6L8, Δ8, and Δ6–9 OmpA peptides in 300 mM SDS-d_{25}/D_2O at pD 2.9 (uncorrected) and 25 °C. The peptides were dissolved, and 1D NMR spectra were recorded after different time intervals. The amide protons are represented by solid boxes, and the height of the boxes reflects the intensity of the corresponding amide resonance observed after the specified exchange time. Ambiguities in the interpretation of the 1D spectra were solved by recording NOESY spectra for the L6L8 peptide, and TOCSY spectra for Δ8 and Δ6–9 (see Experimental Procedures for further details).

results in a similar profile to that observed for the OmpA signal peptide if both signal sequences are aligned in the C-terminus (not shown).[4] The LamB map also includes a "break" in the helix after the hydrophobic core, which coincides with Gly17. Interestingly, Yamamoto and co-workers have found that an idealized signal sequence that directs the secretion of human lysozyme in yeast, Met-Arg-$(Leu)_8$-Pro-Leu-Ala-Ala-Leu-Gly, becomes nonfunctional when the proline residue is substituted by leucine (Yamamoto et al., 1989). A conformational analysis of model peptides representing these and related sequences in TFE/water 1:1 (v/v), using CD and NMR, revealed that lower helicity correlated with higher activity in vivo (Yamamoto et al., 1990). The conformational shift map that can be constructed with the authors' assignments for the functional, proline-containing peptide again shares clear analogy with that observed for the OmpA peptide, with low helicity near the proline and two helical regions, one in the hydrophobic core and another in the C-terminus. The peptide with a Pro → Leu substitution has instead a continuous helix extending through most of the sequence. The authors propose that the signal sequence inserts into the membrane in an α-helical conformation with a bend in the helix and that the C-terminal part of the helix unravels in a later stage upon interaction with the signal peptidase (Yamamoto et al., 1990). Biophysical studies on the PhoE signal sequence led de Kruijff and co-workers to propose a related model where the signal sequence inserts into the membrane, forming a looped helix, with the bend favored by Gly12 (Batenburg et al., 1988a). Additional support for the hypothesis that a bend in the region joining the hydrophobic core and the C-terminus of the signal sequence could have functional importance is given by statistical analysis of the distribution of different types of residues in signal sequences of different species, which shows that turn-promoting residues are particularly abundant at the C-terminal end of the hydrophobic core (von Heijne & Abrahmsén, 1989). It would be interesting to analyze the in vivo activities and conformational properties of mutants of the OmpA, LamB, and PhoE signal sequences, where the mentioned Gly residues were replaced by Pro, a stronger helix breaker, or Leu, a strong helix promoter.

Among the six OmpA peptides studied, three of them, Δ9, Δ8, and I8N, have very similar helical content but very different in vivo activity. Hence, no clear correlation between helicity in TFE/water 1:1 (v/v) and biological activity can be extracted from our results. However, a better correlation between helicity and in vivo activity is obtained when the OmpA peptides are studied in the presence of an interface more closely related to a model membrane, such as SDS micelles. Comparison of the results obtained in TFE/water with those obtained in SDS micelles allows us to distinguish between the intrinsic helical propensities of the peptides and additional conformational effects produced by the interaction with the micelles, effects that correlate with biological activity.

Analysis in SDS Micelles. The analysis of OmpA signal peptides in SDS micelles was more challenging due to the aggregation tendency of some of the peptides and the line broadening observed in some of the data obtained. It is not clear whether the aggregation observed for the WT and I8N peptides involves detergent molecules, but it is certain that it is accompanied by the formation of β structure, as shown by circular dichroism. The line-broadening problem hindered the analysis of the functional L6L8 and Δ9 peptides but, on the other hand, yielded a first indication of their strong association with the micelles. Such association correlates with the in vivo activity of the peptides, as narrower signals were observed for Δ8 and Δ6–9. The possibility that some peptide–peptide interactions contribute to broadening of the NMR signals cannot be discarded, but the observation that the helical contents obtained by NMR are similar to those obtained by CD in much more diluted samples argues that the conformations deduced from the NMR results are independent of the peptide concentration. On the other hand, the stronger association of the functional peptides with the micelles is

[4] The four residues from the mature part of the OmpA protein included in the OmpA peptides studied are not considered in the alignment. The conformational shift map for the LamB signal peptide shows a significantly lower helicity in the C-terminus than that observed in the OmpA peptide, but this difference is most likely due to the end effect produced by the absence of residues from the mature protein at the end of the peptide corresponding to the LamB signal sequence.

consistent with our previous biophysical studies on the OmpA peptides, which showed a clear correlation between biological activity and tendency to interact with phospholipid vesicles (Hoyt & Gierasch, 1991a).

The higher helix content of the functional OmpA peptides in SDS, with respect to that observed in TFE/water, can be rationalized in terms of a combination of electrostatic and hydrophobic interactions. In order to sequester the hydrophobic core from the aqueous environment, this region of the molecule interacts with the hydrophobic chains of the detergent, which leads to the formation of a very stable helix. It is likely that the N-terminal residues are also somewhat buried into the micelles as a consequence of this interaction and the helix propagates through these residues. Such extension of the helix is hindered in TFE/water due to unfavorable electrostatic interactions between the helix dipole and the three positive charges of the N-terminus, but is facilitated in SDS by neutralization of the charges by the negative headgroups of the micelles. Presumably, neutralization of the charges in the N-terminus also occurs for the Δ6–9 peptide, but only a slight increase in the helicity of this region is observed for this peptide; at the same time, the hydrophobic core of Δ6–9 is only a little more helical in SDS than in TFE/water, and the association of this peptide with the micelles is weaker, as judged by the lower degree of line broadening. These observations argue that there is a cooperativity between hydrophobic and electrostatic interactions and that the association of the hydrophobic core with the interior of the micelles plays a major role in the overall increase in helix content observed for the functional peptides.

The critical role of hydrophobicity in the behavior of the OmpA peptides in SDS micelles is underlined by the fact that the functional Δ9 peptide exhibits a higher helicity than the kinetically defective mutant, Δ8, while these two peptides differ only in one residue (Ile versus Ala) and a similar helical content was observed for both peptides in TFE/water. The functional L6L8 mutant is also more helical than Δ8, but the most conspicuous difference between the two peptides lies in the high degree of protection from the solvent of the amide protons of the hydrophobic core in L6L8. Such strong shielding from the aqueous environment is consistent with the existence of a stable helix, but also reflects an additional protection provided by the strong interaction with the hydrophobic chains of the detergent. This conclusion is supported by the observation that the hydrophobic core of the Δ8 peptide is substantially more helical than Δ6–9 and yet a similar accessibility to the solvent is observed for the amide protons of both peptides. The stronger association of the functional peptides with the micelles was also indicated by the line broadening observed in the 1D NMR spectra (see above). A previous analysis of the interactions of LamB and OmpA signal peptides with phospholipid vesicles indicated that only signal peptides with a mean hydrophobicity in the core above a certain threshold are able to penetrate into the acyl region of lipid bilayers (Hoyt & Gierasch, 1991a). The different degrees of association of the OmpA peptides with SDS micelles appear to be another manifestation of the same phenomenon, and their correlation with the results obtained in phospholipid vesicles argues that the conformations observed in SDS are closely related to those adopted by the signal peptides upon interaction with lipid bilayers.

Rather than a specific amino acid sequence, the hallmark of signal peptides is the presence of a hydrophobic core, and recognition of this characteristic led to the proposal of several models of protein export where the signal sequence facilitates protein translocation by direct interaction with the membrane lipids (von Heijne & Blomberg, 1979; Wickner, 1980; Inouye & Halegoua, 1980; Engelman & Steitz, 1981). As mentioned above, several lines of experimental evidence have shown that signal peptides indeed have a high tendency to interact with model membranes (Briggs et al., 1985; Batenburg et al., 1988a; Jones et al., 1990; Killian et al., 1990a,b) and this tendency correlates with their hydrophobicity and with their ability to function in vivo (McKnight et al., 1989; Hoyt & Gierasch, 1991a). Evolutionary arguments also support the view that, at least in primitive cells, protein translocation occurred without the help of any integral membrane proteins (von Heijne & Blomberg, 1979). However, evidence is accumulating in support of models of protein export involving a proteinaceous translocator (Blobel & Doberstein, 1975; Blobel, 1980). Experimental data indicating the existence of protein-conducting channels have been obtained recently (Simon & Blobel, 1991, 1992), and candidates that form or are part of such channels have been proposed both for eukaryotic (Rapoport, 1990; Görlich et al., 1992) and for prokaryotic (Fandl & Tai, 1990; Joly & Wickner, 1993) cells.

Although protein targeting and translocation are mediated by several cytoplasmic and membrane-resident proteins, interactions between signal sequences and membrane lipids can still play an important role in the export mechanism. It is likely that there is a step between the release of the signal peptide from the cytoplasmic targeting protein (SecA in prokaryotes or SRP54 in eukaryotes) and the actual translocation event, which involves passage of the signal sequence into the membrane environment. Our analysis of OmpA signal peptides in SDS micelles argues that, upon interaction with the membrane, signal sequences adopt an α-helical conformation with the hydrophobic core most deeply inserted into the bilayer. Our results also suggest that most of the residues in the OmpA signal sequence spend some time in a helical conformation and, hence, there is a finite probability for the formation of a completely helical structure, which would be long enough to span the bilayer in a transient transmembrane orientation. The relevance to translocation of this biophysical property, which may be common to signal sequences, remains unclear. Insertion of the signal sequence into the membrane will facilitate interaction with the proteinaceous translocator by restricting the search for the translocator to a two-dimensonal diffusion process. The conformational behavior of the signal sequence in a membrane environment as described in this paper may be critical for its productive interaction with the translocation machinery. The results presented here also suggest properties of signal sequences that may be related to their interactions with other hydrophilic/hydrophobic interfaces, such as the binding sites of cytoplasmic proteins that recognize signal sequences.

We next plan to use biophysical methods to study in detail the interactions of signal sequences with components of the export machinery from both prokaryotes and eukaryotes. For this purpose, we will use transferred NOE experiments, which we are currently employing to analyze the conformation of signal peptides upon interaction with phospholipid vesicles. We will also extend our NMR studies in SDS micelles to other signal peptides.

REFERENCES

Bairaktari, E., Mierke, D. F., Mammi, S., & Peggion, E. (1990) *Biochemistry 29*, 10090–10096.

Batenburg, A. M., Demel, R. A., Verkleij, A. J., & de Kruijff, B. (1988a) *Biochemistry 27*, 5678–5685.

Batenburg, A. M., Brasseur, R., Ruysschaer, J.-M., van Scharrenburg, G. J. M., Slotboom, A. J., Demel, R. A., & de Kruijff, B. (1988b) *J. Biol. Chem. 263*, 4202–4207.
Bieker, K. L., Phillips, G. J., & Silhavy, T. J. (1990) *J. Bioenerg. Biomembr. 22*, 291–310.
Blobel, G. (1980) *Proc. Natl. Acad. Sci. U.S.A. 77*, 1496–1500.
Blobel, G., & Dobberstein, B. (1975) *J. Cell Biol. 67*, 835–851.
Briggs, M. S., & Gierasch, L. M. (1984) *Biochemistry 23*, 3111–3114.
Briggs, M. S., & Gierasch, L. M. (1986) *Adv. Protein Chem. 38*, 109–180.
Briggs, M. S., Gierasch, L. M., Zlotnick, A., Lear, J. D., & DeGrado, W. F. (1985) *Science 228*, 1096–1099.
Briggs, M. S., Cornell, D. G., Dluhy, R. A., & Gierasch, L. M. (1986) *Science 233*, 206–208.
Bruch, M. D., & Gierasch, L. M. (1990) *J. Biol. Chem. 265*, 3851–3858.
Bruch, M. D., McKnight, C. J., & Gierasch, L. M. (1989) *Biochemistry 28*, 8554–8561.
Bruch, M. D., Dhingra, M. M., & Gierasch, L. M. (1991) *Proteins: Struct., Funct., Genet. 10*, 130–139.
Bruch, M. D., Rizo, J., & Gierasch, L. M. (1992) *Biopolymers 32*, 1741–1754.
Bruix, M., Perello, M., Herranz, J., Rico, M., & Nieto, J. L. (1990) *Biochem. Biophys. Res. Commun. 167*, 1009–1014.
Chakrabartty, A., Schellman, J. A., & Baldwin, R. L. (1991) *Nature 351*, 586–588.
Chen, Y.-H., Yang, J. T., & Chau, K. H. (1974) *Biochemistry 13*, 3350–3359.
Davis, D. G., & Bax, A. (1985) *J. Am. Chem. Soc. 107*, 2820–2821.
de Vrije, T., de Swart, R. L., Dowhan, W., Tommassen, J., & de Kruijff (1988) *Nature 334*, 173–175.
Dyson, H. J., Rance, M., Houghten, R. A., Wright, P. E., & Lerner, R. A. (1988) *J. Mol. Biol. 201*, 201–217.
Engelman, D. M., & Steitz, T. A. (1981) *Cell 23*, 411–422.
Fandl, J., & Tai, P. C. (1990) *J. Bioenerg. Biomembr. 22*, 369–387.
Geller, B. L., & Wickner, W. (1985) *J. Biol. Chem. 260*, 13281–13285.
Gennity, J., Goldstein, J., & Inouye, M. (1990) *J. Bioenerg. Biomembr. 22*, 233–270.
Gierasch, L. M. (1989) *Biochemistry 28*, 923–930.
Goldstein, J., Lehnhardt, S., & Inouye, M. (1990) *J. Bacteriol. 172*, 1225–1231.
Goldstein, J., Lehnhardt, S., & Inouye, M. (1991) *J. Biol. Chem. 266*, 14413–14417.
Görlich, D., Hartmann, E., Prehn, S., & Rapoport, T. A. (1992) *Nature 357*, 47–52.
Greenfield, N., & Fasman, G. D. (1969) *Biochemistry 8*, 4108–4116.
Hartl, F.-U., Lecker, S., Schiebel, E., Hendrick, J. P., & Wickner, W. (1990) *Cell 63*, 269–279.
Henry, G. D., & Sykes, B. D. (1990) *Biochemistry 29*, 6303–6313.
Hoyt, D. W., & Gierasch, L. M. (1991a) *Biochemistry 30*, 10155–10163.
Hoyt, D. W., & Gierasch, L. M. (1991b) *J. Biol. Chem. 266*, 14406–14412.
Inouye, M., & Halegoua, S. (1980) *CRC Crit. Rev. Biochem. 7*, 339–371.
Jeener, J., Meier, B. H., Bachmann, P., & Ernst, R. R. (1979) *J. Chem. Phys. 71*, 4546–4553.
Jiménez, M. A., Nieto, J. L., Herranz, J., Rico, M., & Santoro, J. (1987) *FEBS Lett. 221*, 320–324.
Joly, J. C., & Wickner, W. (1993) *EMBO J. 12*, 255–263.
Jones, J. D., McKnight, C. J., & Gierasch, L. M. (1990) *J. Bioenerg. Biomembr. 22*, 213–232.
Kendall, D. A., & Kaiser, E. T. (1988) *J. Biol. Chem. 263*, 7261–7265.
Kendall, D. A., Bock, S. C., & Kaiser, E. T. (1986) *Nature 321*, 706–708.
Killian, J. A., de Jong, A. M. Ph., Bijvelt, J., Verkleij, A. J., & de Kruijff, B. (1990a) *EMBO J. 9*, 815–819.
Killian, J. A., Keller, R. C. A., Struyvé, M., de Kroon, A. I. P. M., Tommassen, J., & de Kruijff, B. (1990b) *Biochemistry 29*, 8131–8137.
Kumar, A., Wagner, G., Ernst, R. R., & Wüthrich, K. (1981) *J. Am. Chem. Soc. 103*, 3654–3658.
Lehnhardt, S., Pollitt, S., & Inouye, M. (1987) *J. Biol. Chem. 262*, 1716–1719.
Mammi, S., & Peggion, E. (1990) *Biochemistry 29*, 5265–5269.
Marqusee, S., Robbins, V. H., & Baldwin, R. L. (1989) *Proc. Natl. Acad. Sci. U.S.A. 86*, 5286–5290.
McKnight, C. J., Briggs, M. S., & Gierasch, L. M. (1989) *J. Biol. Chem. 264*, 17293–17297.
McKnight, C. J., Rafalski, M., & Gierasch, L. M. (1991) *Biochemistry 30*, 6241–6246.
Nelson, J., & Kallenbach, N. (1989) *Biochemistry 28*, 5256–5261.
O'Neil, J. D. J., & Sykes, B. D. (1989) *Biochemistry 28*, 699–707.
O'Neil, K. T., & DeGrado, W. F. (1990) *Science 250*, 646–651.
Padmanabhan, S., Marqusee, S., Ridgeway, T., Laue, T. M., & Baldwin, R. L. (1990) *Nature 344*, 268–270.
Pardi, A., Wagner, G., & Wüthrich, K. (1983) *Eur. J. Biochem. 137*, 445–454.
Pastore, A., & Saudek, V. (1990) *J. Magn. Reson. 90*, 165–176.
Randall, L. L., & Hardy, S. J. S. (1989) *Science 243*, 1156–1159.
Rapoport, T. A. (1986) *CRC Crit. Rev. Biochem. 20*, 73–137.
Rapoport, T. A. (1990) *Trends Biochem. Sci. 15*, 355–358.
Rohl, C. A., Scholtz, J. M., York, E. J., Stewart, J. M., & Baldwin, R. L. (1992) *Biochemistry 31*, 1263–1269.
Schatz, P. J., & Beckwith, J. (1990) *Annu. Rev. Genet. 24*, 215–248.
Siegel, V., & Walter, P. (1988) *Trends Biochem. Sci. 13*, 314–316.
Simon, S. M., & Blobel, G. (1991) *Cell 65*, 371–380.
Simon, S. M., & Blobel, G. (1992) *Cell 69*, 677–684.
Szilágyi, L., & Jardetzky, O. (1989) *J. Magn. Reson. 83*, 441–449.
Tanji, Y., Gennity, J., Pollitt, S., & Inouye, M. (1991) *J. Bacteriol. 173*, 1997–2005.
Verner, K., & Schatz, G. (1988) *Science 241*, 1307–1313.
von Heijne, G. (1985) *J. Mol. Biol. 184*, 99–105.
von Heijne, G., & Blomberg, C. (1979) *Eur. J. Biochem. 97*, 175–181.
von Heijne, G., & Abrahmsén, L. (1989) *FEBS Lett. 244*, 439–446.
Wickner, W. (1980) *Science 210*, 861–868.
Williamson, M. P. (1990) *Biopolymers 29*, 1423–1431.
Wishart, D. S., Sykes, B. D., & Richards, F. M. (1991) *J. Mol. Biol. 222*, 311–333.
Wishart, D. S., Sykes, B. D., & Richards, F. M. (1992) *Biochemistry 31*, 1647–1651.
Wüthrich, K. (1986) *NMR of Proteins and Nucleic Acids*, Wiley, New York.
Yamamoto, Y., Taniyama, Y., Kikuchi, M., & Ikehara, M. (1987) *Biochem. Biophys. Res. Commun. 149*, 431–436.
Yamamoto, Y., Taniyama, Y., & Kikuchi, M. (1989) *Biochemistry 28*, 2728–2732.
Yamamoto, Y., Ohkubo, T., Kohara, A., Tanaka, T., Tanaka, T., & Kikuchi, M. (1990) *Biochemistry 29*, 8998–8906.